■ Materials Science inc. Nanomaterials & Polymers

A Synaptic Electrochemical Memristor Based on the Cu^{2+}/Zn^{2+} Cation Exchange in Zn:CdS Thin Films

Mirko Congiu,*[a] Miguel H. Boratto,[b] and Carlos F. O. Graeff[c]

Neuromorphic hardware systems that simulate functions of biological brain synapses have been widely investigated due to their possible application in brain-inspired computing. We hereby report on a novel electrochemical state machine based on Zn:CdS thin films. The memory switching mechanism involves the cation exchange of Cu^{2+} and Zn^{2+} acting as inorganic "neurotransmitters". Similarly to the synapse-neurotransmitter interactions, Cu^{2+} ions increase the conductivity and the electrocatalytic activity of Zn:CdS towards the ferrocene/ferrocenium redox process. The cationic substitution of Zn^{2+} by Cu^{2+} in the film has shown significant changes in the electrochemical characteristic of the device. Such effects have been investigated with both alternated current (impedance) and direct current (voltammetry and I vs V) measurements. The cation exchange mechanism allows to write and store an electrochemical information into the device. Such information can be gradually erased by exchanging the absorbed Cu^{2+} ions with Zn^{2+}. By means of a timed soaking, of the active area, with Cu^{2+} and Zn^{2+} diethyldithiocarbamates, the device can be driven through multiple conduction states, making it suitable for applications in artificial synapses research and memory storage systems.

1. Introduction

The huge amount of data produced nowadays by modern computing technologies is bringing silicon-based memory data processing technology to its limits. In fact, most data processing systems are based on (flash) memory cells arrays which can store volatile information just in the binary form (i.e. bits 0 or 1). Nevertheless, most of the raw information registered and stored for general purposes are not binary. For example, the response of a typical sensor is generally an analogic value (e.g. resistance, conductibility etc.); such information must be digitized before being stored in a flash memory, consuming time, energy and space.[1] In this direction, the interest of the scientific community to develop alternative non-volatile technology such as memristors (memory resistors) it's still growing. In 1971, Chua et al. proposed, to the scientific community, the theory on nonlinear circuits, describing the memristor (MEM), a passive element capable to fill the mathematical relationship between the charge Q(t) and the current flux J(t).[2] The first "real" memristor was finally discovered in 2008 by the HP labs research team.[3] Basically, a memristor is a device that may present thousands of analogic memory levels, allowing the storage of dense and complex information.[4,5] This capability is very interesting in the field of advanced electronic applications such as: computing and logic operations,[6,7] neuromorphic computing[8,9] and analog circuits.[10] New concepts about MEMs have been developed, so far in the literature, especially in reconfigurable logic.[6,11–13] Several evidences have demonstrated that MEMs are strong candidates for frontier data processing electronics, capable to store complex information. Thus, MEMs are considered crucial elements for artificial intelligence systems.[14] Besides the importance of memristors, recently, organic electrochemical transistors have been demonstrated to be capable of simulating brain's synaptic cells.[15–17]

In a biologic neural network, a neuron transfers the information to a second neuron through an axon terminal, connected by several synapses to dendrites of the second neuron. The neural network is created by the formation of trillions of synaptic connections between neurons. Specific channels for positive ions (i.e. Na$^+$), activated by neurotransmitters, modulate the membranes potential transferring the electrical information through axons terminals to other neurons or to another target cell. The information flows from the pre-synaptic to the post-synaptic cell. These connections form a highly interconnected network based on "plastic" links between the neurons. The plasticity of the connection is a fundamental concept in biology and is related to the learning capability of the brain .[18,19] Considering the high complexity of a biologic neural network, it is difficult to be emulated using conventional electronics. One of the first emulation attempt was based on an electrical circuit for the simulation of the giant squid axon. This circuit is also known as the Hodgkin–Huxley model.[20] The model considers the cell's membrane as a capacitive element, where the sodium and potassium channels are represented as two voltage-driven variable resistors. The

[a] Dr. M. Congiu
UNESP – São Paulo State University, School of Sciences, POSMAT – Post-Graduate Program in Materials Science and Technology, Av. Eng. Luiz Edmundo Carrijo Coube 14–01, 17033-360, Bauru, SP, Brazil
E-mail: mirko.congiu@fc.unesp.br

[b] Dr. M. H. Boratto
Federal University of Santa Catarina (UFSC), Department of Physics, Post-Graduate Program in Physics, Florianópolis, SC, 88040-900, Brazil

[c] C. F. O. Graeff
UNESP – São Paulo State University, School of Sciences, Department of Physics, Av. Eng. Luiz Edmundo Carrijo Coube 14–01, 17033-360 Bauru, SP, Brazil

original model considers that each cell is connected by dissipative resistances, responsible for the pulse transmission along the chain (axon). Recently Chua *et. al* have described an alternative model in which the voltage driven resistances, of the original model, were replaced by two memristors.[21] This model explains the anomalous behaviors of the Hodgkin–Huxley model, i.e. the lack of rectifiers as well as the lack of inductances as analyzed by Cole and Baker.[22,23]

In this work we have investigated the electrochemical behavior of Cu-doped Zn:CdS thin films treated with different chemical solutions: one based on Cu^{2+} which rapidly increases the Cu-content in the films, and another one, based on Zn(II) diethyldithiocarbamate which removes Cu^{2+} replacing it with Zn^{2+}. The effects of the ionic exchange were studied in both AC and DC modes using two different setups. For AC measurements, the electrochemical impedance spectroscopy was used in a ferrocenium/ferrocene redox pair (FCE) based electrolyte. While, in DC mode, the Zn:CdS film was measured using two electrical contacts. As discussed above, a synapse is a biological structure which permits a neuron to pass an electrical or chemical information to another neuron or to another target cell.[24] Different processes are involved in the transmission of information, e.g. the liberation of specific neurotransmitters which activates voltage-gated Ca^{2+} channels.[25] The as mentioned processes are activated or inhibited by specific neurotransmitters that are released into the extracellular fluid and bind to specific receptors on the synapse membrane. In a very similar way, Zn:CdS thin films act as a synthetic synapse in which Zn^{2+} centers behave as ion-exchange receptors for Cu^{2+}. This cation exchange influences the electrical and electrochemical behaviors of the thin films. The amount of the exchanged Cu^{2+} can easily drive the film's electrical resistance to a low value, passing through a *continuum* of different states. Then, the device can be chemically reset to its initial resistance state by removing Cu^{2+} and replacing it with Zn^{2+}. Through simple experiments we demonstrate the potentiality of this ion-exchange system in an alternative Hodgkin–Huxley model based on Zn:CdS memristors controlled by microfluidics.

2. Results and discussion

Electrochemical Characterization

In our setup, the Zn:CdS films represent the working electrode while a Pt wire was used as counter electrode in a typical two-electrode electrochemical cell configuration. The electrolyte of the cell is based on a solution of ferrocene (Fc) and its respective oxidized form ferrocenium cation (Fc^+). Virgin (VGN) Zn:CdS electrodes were submitted to EIS analysis prior to any operation in order to determinate the initial electrochemical memory state. The electrocatalytic activity of the surface was considered as a multiparametric memory information, calculated by fitting the EIS spectrum with an equivalent circuit. In figure 1, one can see a typical impedance spectrum of a VGN Zn:CdS electrode (Zn 10 at%) in FCE electrolyte. The equivalent circuit of the electrochemical interface consists of a series resistance (Rs) which represents the contributions of the wires
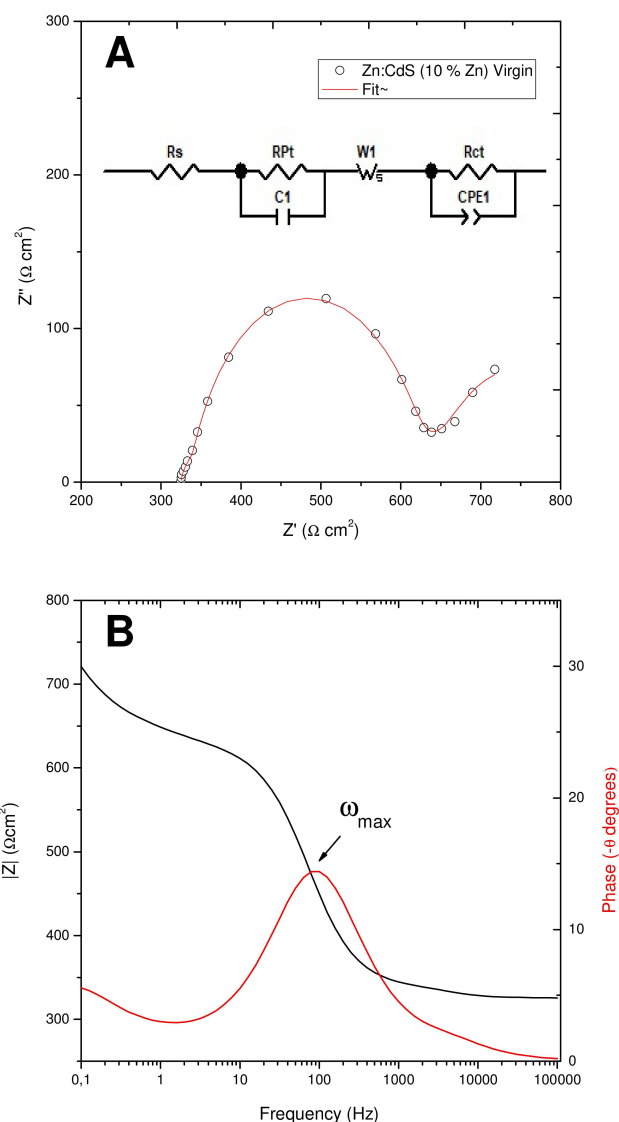

Figure 1. a) Nyquist plot of the impedance response of a typical as prepared (virgin, VGN) Zn:CdS (10% Zn) electrode immersed in FCE electrolyte. b) The Bode plot presents the frequency response of the electrochemical system (RC) from 0.1 Hz to 100 kHz.

and the FTO/Zn:CdS sheet resistance; an RC system representing the electrochemical interface between the Pt wire counter electrode and FCE; and a Warburg-short diffusion element (Ws) representing the ionic diffusion of Fc^+ through the electrochemical cell. To represent the interface between Zn:CdS and FCE, a constant phase element (CPE) was used instead of a regular capacitor considering the roughness of the film's surface. From the Nyquist plot, (Figure 1 a) one can notice the characteristic shape of a system composed from two series RC systems. The first small semicircle (325-350 Ωcm^2) is related to the charge-transfer process at the CE interface. As Pt is highly catalytic for the oxidation/reduction of ferrocene/ferrocenium redox couple,[26] it showed a low charge transfer resistance (10.2 $\pm$ 0.5 Ωcm^2) and a capacitance of 3.5 $\pm$ 0.3 μF. On the other side of the cell, the Zn:CdS//FCE interface presents a

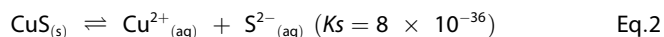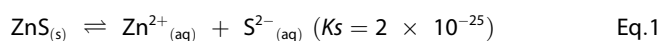higher resistive component returning a value of Rct of 279.4 ± 1.5 Ωcm² and a capacitance of 8.5 ± 0.5 μF.

From the Bode plot, Fig.1 b, the maximum value of imaginary impedance in Figure 1a, can be related to the maximum recombination frequency (ω_{max}) or the time constant (τ) of the electrochemical system.[27] As can be seen, the maximum phase angle frequency in VGN electrodes is around 100 Hz. This frequency is related to the time constant of the RC electrochemical system, which represents both the speed of the charge-discharge of the capacitive interface between electrode and electrolyte, and the speed of the redox reaction.[28,29] To set the system to the low resistance state (LRS) the electrode was dipped into a 0.1 M Cu(NO₃)₂ solution (MeOH). We used MeOH rather than water for both the LRS activation and the washing step to ensure a fast drying, avoiding the absorption of water which might interfere with the electrical measurements.

When the VGN Zn:CdS electrode is dipped in the copper nitrate solution, a fast cation exchange reaction occurs leading to a visible change in the optical properties of the film. In fact, the film rapidly changes its color from pale yellow to light brown, due to the substitution of Zn^{2+} by Cu^{2+} or in the conventional notation, Cu_{Zn}. The optical change induced by the cation substitution is shown in the transmittance spectra (Figure 2).
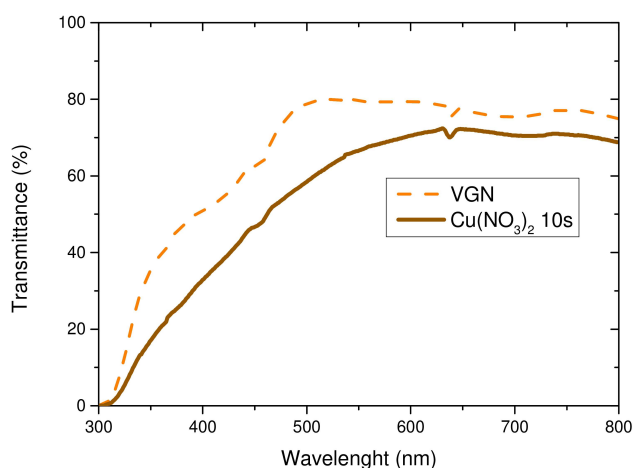

Figure 2. Transmittance spectra of a virgin (VGN) Zn:CdS electrode before and after the treatment with the 0.1 M Cu^{2+} solution in methanol. The effect of the chemical substitution of Zn by Cu leads to a decrease of the transmittance with the formation of a broad absorption band at lower wavelengths.

The substitution of Zn^{2+} by Cu^{2+} changes the transmittance of the film and a new broad absorption band appears at lower wavelengths; at 500 nm a reduction of the optical transmittance from 80 to 60% is observed. This may occur due to the formation of lower energy states induced by Cu^{2+} inside the Zn:CdS bandgap, as reported also by Ortiz-Ramos et al..[30] Equations 1 and 2, describe the cation exchange process.

$$ZnS_{(s)} \rightleftharpoons Zn^{2+}_{(aq)} + S^{2-}_{(aq)} \ (Ks = 2 \times 10^{-25}) \qquad \text{Eq.1}$$

$$CuS_{(s)} \rightleftharpoons Cu^{2+}_{(aq)} + S^{2-}_{(aq)} \ (Ks = 8 \times 10^{-36}) \qquad \text{Eq.2}$$

The clear difference in water-solubility (Ks) of ZnS and CuS can be explained considering the electronegativity of copper and zinc, 1.90 eV and 1.65 eV respectively. Notice that the electronegativity of sulfur is 2.58 eV so the Cu–S bond have a higher covalent character in comparison with Zn–S. In fact, the latter is more polar due to the higher electronegativity difference (between the chalcogenide and the metal). The electronegativity difference between Zn and S (Δ_{EN}) is 0.93 eV and 0.68 between Cu and S. Accordingly to the commonly used convention, both Zn–S and Cu–S bonds can be classified as polar covalent however the Zn–S bond is more polar than Cu–S due to the higher Δ_{EN}. Thus, the electronegativity difference can be considered as an index of polarity of a chemical bond and thus the tendency of a molecule to be more soluble than another into a polar solvent such as water. However, this is not the sole reason of the huge solubility difference between CuS and ZnS. Nevertheless, the different stability of the metal-chalcogenide bond due to the π back-bonding stabilization is another parameter that should be considered. This effect is, basically, the unexpected electron transfer from the positive-charged metal center (M^{2+}) to the unoccupied d orbital of the ligand (S^{2-}).[31,32] Transition metals sulfides normally shown a poor solubility in polar solvent due to the participation of d orbitals in the bond between the metal and the chalcogenide (i.e. S). Such phenomenon is particularly relevant in metals such as Cu, Ag and Hg while becomes of minor importance for Zn, Cd and post-transition elements. In fact, the energy of their d orbitals is already so low to further stabilize the bond with the chalcogenide.[33,34] Considering the values of Ks, given in Eq. 1 and 2, ZnS is 1.6 x 10⁵ times more soluble than CuS. For this reason, the overall equilibrium is completely shifted in the direction of CuS formation when both Zn^{2+} and Cu^{2+} are in solution. This reaction is well known and was recently used to grow nanostructures of CuS starting from a sacrificial ZnS template.[35] Besides the electrical behavior of the Cu^{2+} treated films show significant changes. Both AC and DC measurements used the experimental setup described earlier. In Figure 3 the one can see the voltammogram of Zn:CdS electrode before (VGN) and after the treatment with Cu(NO₃)₂ (LRS). The voltammogram of the VGN electrode showed a lower current density over the entire voltage range. Furthermore, the voltammogram of VGN shown a behavior typical of irreversible redox systems.

In the first part of the CV, between 0 V and 0.4 V, the VGN electrode presents quasi-ohmic behavior. As the slope of the current (I) vs voltage plot represents the inverse of the electrical resistance (R^{-1}) of the interface, one can see that the slope of the cathodic part of the voltammogram (I > 0) is higher than that of the anodic part (I < 0). Thus, the electron-transfer process is more effective than the hole-transfer in this interface. This effect can be explained considering that $Zn_{1-x}Cd_xS$ normally exhibit a n-type semiconducting behavior.[36,37] So, when the working electrode is forward biased (cathode), the
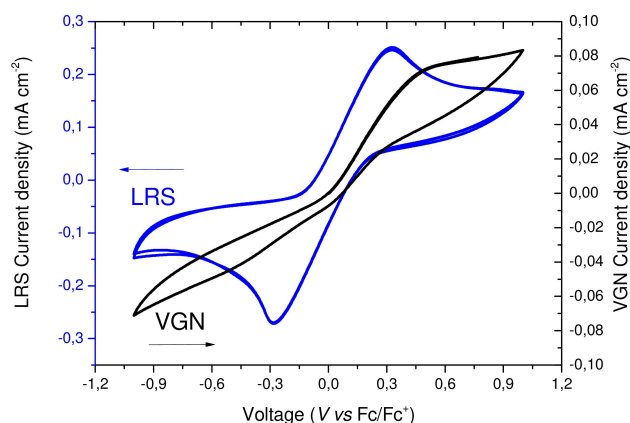
Figure 3. Cyclic voltammetry (CV) of the same electrode before (VGN) and after (LRS) treatment with Cu^{2+} 0.1 M. VGN electrode shows a typical pattern of an irreversible redox system, while the LRS activated electrode presents a completely reversible system for the redox pair in solution (FCE). The measurement was performed from 1 to −1 V at 100 mVs^{-1} scan rate.

charge carriers are pulled from the bulk to the interface and transferred to the electrolyte (reduction of Fc^+). On the other hand, in the negative part of the curve, the working electrode (anode) is in reverse bias regime, in which the electrons are withdrawn from the interface into the VGN Zn:CdS electrode, which presents a higher resistance and is responsible for the irreversibility of the redox process on this electrode.

The cyclic voltammogram changes when the film is treated with the LRS activating solution. The shape of the voltammo-gram is typical of reversible reactions, i.e. the Cu-doped Zn:CdS electrode is capable to oxidize and reduce Fc/Fc^+. It is possible to see two well-defined peaks, the cathodic at 0.33 V with a peak current density of 0.232 mA cm^{-2}, and the anodic at −0.28 V with a current density of −0.230 mA cm^{-2}. Such increase in the electrocatalytic activity of the working electrode after the cation exchange reaction was analyzed also by electrochemical impedance spectroscopy. As reported in Table 1, after the treatment with Cu^{2+} and washing with pure methanol, the as obtained Zn(Cu):CdS interface showed a significant increase in the electrocatalytic activity (lower Rct).

The value of the charge transfer resistance decreased from an initial value of 279.4 ± 1.6 Ω cm^2 (VGN) to 27.7 ± 2.3 Ω cm^2, while the interfacial capacitance remained around the initial value (6.7 ± 1.2 μF). In a recent paper from our research group,[38] films of pure CuS have also shown high catalytic properties in this redox process. Considering the system as a synthetic synapse, Cu^{2+} behaves as a neurotransmitter that increases the conductivity of the memory cell. The initial resistance state can be chemically restored by replacing Cu^{2+} ions with Zn^{2+}. To perform the chemical substitution, the films were dipped into a saturated solution of $Zn(Et_2DTC)_2$ in $CHCl_3$.

At the starting time, the system is set to LRS and its charge transfer resistance is very low (27.7 ± 2.3 Ωcm^2). The following processes to set the cell to HRS is performed in the Cu-removal solution which promotes the withdrawal of Cu^{2+} from the film, leading to a lower electrocatalytic activity (increasing Rct). As reported in Table 1, the longer dipping-time in $Zn(Et_2DTC)_2$ solution leads to higher Rct values, and the electrochemical system gradually becomes less active towards the Fc/Fc^+ redox process. This effect is due to the increase of Zn^{2+} into the film, which reduces the number of active sites where the electro-chemical reaction is energetically favorable. The increase in Rct can be seen in Figure 4. The plots of Fig.4b represent the impedance response of the electrochemical interface Zn(Cu):CdS//FCE//Pt after different dipping times into $Zn(Et_2DTC)_2$. During the dipping, Zn^{2+} replaces Cu^{2+} in the films, leading to a gradual increase of the semicircles amplitude (Rct value).

After dipping the electrode for 30 minutes, in Cu-removal solution, the system reaches a value of Rct close to that of VGN electrodes. The effect of the Cu-removal treatment is visible also in the frequencies domain as shown in Figure 4a. The longer dipping time leads to lower ω_{max} of the RC system, which decreases the redox process kinetics at the electrode/electrolyte interface.[29] Although, the electrode showed a Rct value close to the initial VGN while ω_{max} remains higher than that of VGN. This could be due to the presence of residual Cu^{2+} ions trapped in deep regions inaccessible by the solution. As discussed in the next section, the removal of Cu^{2+} and its subsequent substitution by Zn^{2+} is promoted by $Zn(Et_2DTC)_2$. Probably the high dimension of the zinc diethyldithiocarba-mate molecule hinders it to diffuse deeply into the film. Thus,

Table 1. Resume of the fitted electrochemical parameters of the Zn:CdS electrodes after different operations. In this experiment the chemical treatment with Cu^{2+} 0.1 M was considered as the writing operation (W) while the Cu-removal process the erasing (E). (*) Once the electrochemical characteristics of the films returned to a condition close to the VGN state, the sample was once more dipped in the Cu^{2+} solution to induce the electrode to the LRS (W). (**) Notice that the time values listed in this column are referred to the duration of each dipping of the device in the Cu-removal solution (E); i.e. the device is erased for 5 minutes, characterized and dipped again in the Cu-removal solution. At the end of the sixth erasing operation, the device reaches a total erasing time of 30 minutes, as the sum of each erasing operation.

| Operation	Solution	Time** (min)	State	Rs (Ωcm^2)	R$_{Pt}$ (Ωcm^2)	C$_{Pt}$ (μF)	R$_{CT}$ (Ωcm^2)	C$_{Zn:CdS}$ (μF)
-	-	0	VGN	325.1 ± 0.2	10.2 ± 0.4	3.5 ± 0.3	279.4 ± 1.6	8.5 ± 0.5
W	Cu^{2+} 0.1 M	0.16	LRS	324.5 ± 0.3	8.3 ± 1.8	4.5 ± 1.8	27.7 ± 2.3	6.7 ± 1.2
E	$Zn(Et_2DTC)_2$	5	HRS 1	327 ± 0.3	8.5 ± 0.7	3.9 ± 1.6	31.2 ± 1.5	5.8 ± 0.9
E	$Zn(Et_2DTC)_2$	5	HRS 2	325.4 ± 0.3	8.7 ± 2.8	3.5 ± 0.9	37.0 ± 3.3	4.3 ± 0.4
E	$Zn(Et_2DTC)_2$	5	HRS 3	329.6 ± 0.4	11.0 ± 2.9	3.0 ± 0.6	53.1 ± 3.3	3.7 ± 0.3
E	$Zn(Et_2DTC)_2$	5	HRS 4	333.4 ± 0.3	9.8 ± 2	3.9 ± 0.5	100.4 ± 2.5	2.3 ± 0.1
E	$Zn(Et_2DTC)_2$	5	HRS 5	336.5 ± 0.3	8.3 ± 1.1	4.6 ± 0.5	167.9 ± 1.7	3.2 ± 0.1
E	$Zn(Et_2DTC)_2$	5	HRS 6	327.0 ± 0.4	10.1 ± 1.2	4.6 ± 0.6	270.0 ± 2.2	3.5 ± 0.2
W*	Cu^{2+} 0.1 M	0.16	LRS	335.6 ± 0.3	9.7 ± 2.3	5.3 ± 0.2	22.2 ± 2.9	7.3 ± 2.5
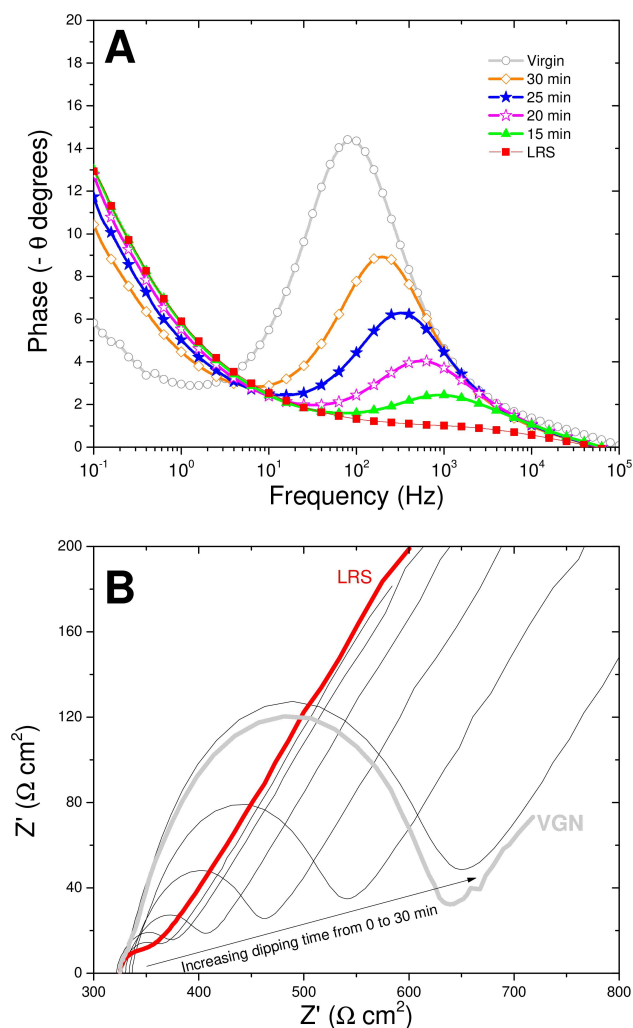
Figure 4. Erasing process of a VGN electrode initially set to LRS by dipping in Cu^{2+} 0.1 M solution. The erasing process was performed through different dipping-times in Cu-removal solution, during up to 30 minutes. Successive EIS measurement were performed after 5 minutes of device dipping in Cu-removal solution until the value of the charge-transfer resistance (Rct) was close to that of VGN. (a) Phase angle (- degrees) as a function of modulation frequency. It can be seen a progressive decrease of the peak frequency (ω_{MAX}) at longer dipping-time in Cu-removal solution. (b) Successive Nyquist plots, as function of the dipping time in Cu-removal solution, which also shows an increase on the Rct values for longer dipping-time in Cu-removal solution.

some regions could remain catalytically active, leading to a higher value of ω_{max} in comparison whit VGN. So the presence of copper in the film might be the cause of the different values of the double layer capacitance of Zn:CdS (Tab. 1) observed in VGN (8.5 ± 0.5 μF) and in erased devices (3.5 ± 0.2 μF). The reaction with $Cu(Et_2DTC)_2$ modifies the dielectric properties of the device and this could explain the capacitance difference between the VGN and the erased ones. This effect could be advantageously used to distinguish real VGN devices from the erased ones. The small difference in the capacitance of the platinum counter-electrode could be probably due to the absorption of metal ions on the surface during writing and

erasing operations. Nevertheless, the remaining concentration of Cu^{2+} does not contribute to the overall films conductivity; this could explain the higher value of Rct after 30 minutes soaking in Cu-removal solution.

The chemical reaction that removes Cu^{2+} ions from Zn(Cu): CdS films, replacing them with Zn^{2+} is mediated by the diethyldithiocarbamate (DTC) complex dissolved in chloroform, and can be described by equation 3.

$$Zn(Et_2DTC)_2 + Cu_{(Zn)}:CdS(s) \rightleftharpoons Cu(Et_2DTC)_2 + Zn:CdS(s) \qquad \text{Eq.3}$$
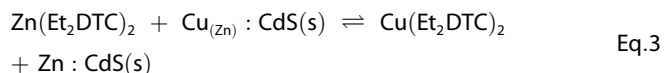
When the saturated solution of $Zn(Et_2DTC)_2$ wets the film's surface, the Zn complex reacts with the Cu^{2+} centers promoting the ionic exchange. The electrode changes its electrical resistance, due to the partial substitution of Cu^{2+} by Zn^{2+}. In this case the use of a non-polar solvent is mandatory. In fact, it is important to consider that a polar solvent stabilizes ions such as S^{2-}, Cu^{2+} and Zn^{2+} that could shift the equilibrium to the formation of CuS due to the huge solubility difference with respect to ZnS. By using a non-polar solvent, the ions solvation will be neglectable and thus the difference in solubility of ZnS and CuS does not affect the overall equilibrium.

The formation of $Cu(Et_2DTC)_2$ was confirmed through a simple experiment: first, the UV-Vis absorption of a $Zn(Et_2DTC_2)_2$ solution in chloroform was performed; subsequently, the activated electrode (containing Cu), was dipped in the solution for 50 minutes. After the reactions presented in equation 3 occurred, the spectrum of the solution was again recorded for comparison with the pure $Zn(Et_2DTC_2)_2$ solution, before the film dipping. Figure 5 presents the UV-Vis absorbance performed in
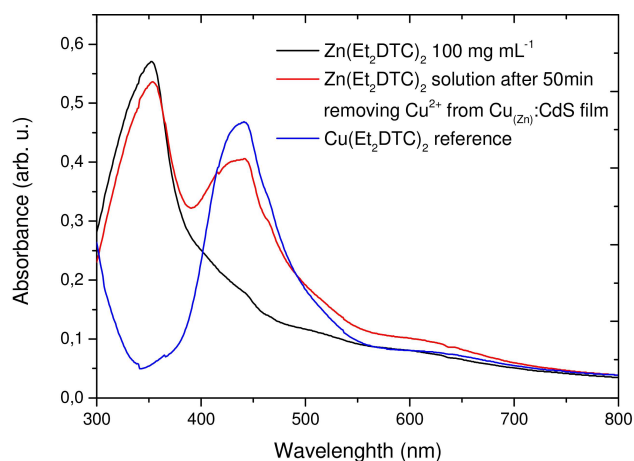
Figure 5. Absorbance spectra of the Cu-removal solution before (black line) and after (red line) dipping. The extraction of the substituted Cu ions from the Zn:CdS electrode, mediated by $Zn(Et_2DTC)_2$, is confirmed by the formation of $Cu(Et_2DTC)_2$ inside the $Zn(Et_2DTC)_2$ solution. The blue line plot represents the absorption spectra of $Cu(Et_2DTC)_2$ in chloroform for reference.

the solutions before and after $Cu_{(Zn)}$:CdS dipping. The starting solution showed the typical absorption spectrum of Zn

(Et$_2$DTC)$_2$ with a broad peak presenting a maximum at 351 nm without any further absorption peaks. After film dipping, the spectrum presented a new peak at 440 nm and a reduction in the intensity of the Zn(Et$_2$DTC)$_2$ peak. By comparing the as obtained spectrum with a reference solution of Cu(Et$_2$DTC)$_2$, it is obvious that the peak at 440 nm belongs to the copper complex's. This result demonstrates that the removal of copper from the activated electrodes leads to the formation of the respective diethyldithiocarbamate complex. Notice that in this experiment we used a diluted solution of Zn(Et$_2$DTC)$_2$ (100 mg mL^1), instead of the saturated one, to avoid the saturation of the absorption spectrum. For this reason, we extended the reaction time up to 50 minutes to ensure the formation of detectable concentration of Cu(Et$_2$DTC)$_2$ in the solution. Similar results were obtained using Cd(Et$_2$DTC)$_2$ as Cu-removal. In this case the removed copper complexes in the film are replaced by Cd's (see supplementary figure S2).

The removal of Cu^{2+} occurs due to the different stability of the DTC complexes. For instance, the stability constants (logβ_1 and logβ_2) of Cu(Et$_2$DTC)$_2$ in methanol are 11.7 and 23.9 respectively, while the same constants for Zn(Et$_2$DTC)$_2$ are 7.7 and 15.1.[39] The stability constants (β_1 and β_2) of a diethyldithiocarbamate complex of a bivalent metal (M^{2+}) can be written as follows (Eq. 4 and 5):

$$\beta_1 = \frac{[Me(Et_2DTC)_2]}{[MeEt_2DTC^+][Et_2DTC^-]} \qquad \text{Eq.4}$$

$$\beta_2 = \frac{[MeEt_2DTC^+]}{[Me^{2+}][Et_2DTC^-]} \qquad \text{Eq.5}$$

By comparing β_1 and β_2 of Zn and Cu diethyldithiocarbamates, it is explicit that the equilibrium of equation 3 is shifted to right. Notice that also Cd^{2+} forms a stable complex with Et$_2$DTC$^-$ ligand. The complex Cd(Et$_2$DTC)$_2$ is slightly more stable than Zn(Et$_2$DTC)$_2$ (logβ_1 = 8.4; logβ_2 = 16.7).[39] Thus, when all the solvent-accessible Cu^{2+} is removed from the film, Zn(Et$_2$DTC)$_2$ could react with Cd^{2+} leading to the formation Cd(Et$_2$DTC)$_2$. Therefore, it is important to halt the ion-exchange process when Rct reaches a value close to that of VGN electrodes, to avoid the inclusion of a quantity of Zn^{2+} higher than the initial atomic concentration (10%). Compositional analysis, performed through EDX (S.I. Figure S3-S5), indicates the probable coexistence of both equilibria, showing a slight reduction of the Cd peak intensity just after the film treatment with Zn(Et$_2$DTC)$_2$ (Figure S5). Morphological studies of the film's surface after was performed through Confocal microscopy and is presented in Figure S6 in the supplementary information. The results have shown that slight roughness changes occur on the film surface after treatment in Zn(Et$_2$DTC)$_2$ and Cu(NO$_3$)$_2$ solutions.

From AC measurements to a DC state-sensing approach

The synaptic activation effect of Cu^{2+} can be measured also through electrical measurements. This alternative sensing approach utilizes the differences, in electrical resistance, caused by the cationic exchange of Cu^{2+} and Zn^{2+} at the interface Zn: CdS//solution. Previously, we have presented the equivalent electrical circuit corresponding to the electrochemical cell Cu$_{(Zn)}$:CdS//FCE//Pt (Figure 1 a). The resistive element Rct represents the charge transfer resistance at the interface between the working electrode (Zn:CdS) and the liquid electrolyte (FCE). For DC measurements the considered system is constituted only by the Zn:CdS thin film, approximable to a resistive element between two electrodes (FTO) placed at a fixed distance of 1 mm (inset of Figure 6). Such configuration
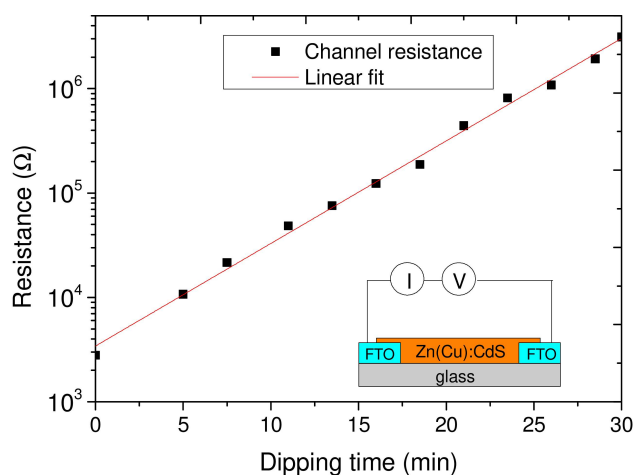
Figure 6. Evolution of the channel resistance as function of the dipping-time in the Cu-removal solution after the LRS setting of the Zn:CdS thin film based device. The DC setup is represented in the inset of the figure.

can be considered a solid neuromorphic device, like the artificial synapse discussed in the previous section. The as-proposed devices work similarly to electrochemical transistors [17,40] in which the conduction through the channel is modulated by ion exchanges rather than gate-voltage sweeps.

The electrical setup was obtained by corroding the FTO with Zn powder and concentrated HCl using a protective mask, following a procedure in the literature.[41] The electrical characterization was initially performed to obtain the electrical resistance of the VGN sample, which presented values ranging 1 to 3 MΩ. Then, the electrode was activated to LRS using the Cu^{2+} 0.1 M solution, and the resistance was measured (2801.8 Ω). Similarly, to previous experiments, the electrode was treated with the Cu-removal solution and the channel resistance was measured at fixed time intervals (2.5 min). The different values of resistance states are presented in figure 6.

The channel resistance (Figure 6) has shown an exponential increase as a function of the dipping-time (Cu-removal solution). The electrical resistance, the following condition is verified:

$$\frac{\partial \log(R_{channel})}{\partial t} = k \qquad \text{Eq.6}$$

where $R_{channel}$ is the channel resistance, t is the dipping-time in

the Cu-removal solution and k is a constant. By performing a linear fit, the value of $k = 0.098$ was calculated.

The evaluation of Zn:CdS films working as artificial synapses is presented in figure 7. The results have shown that the device
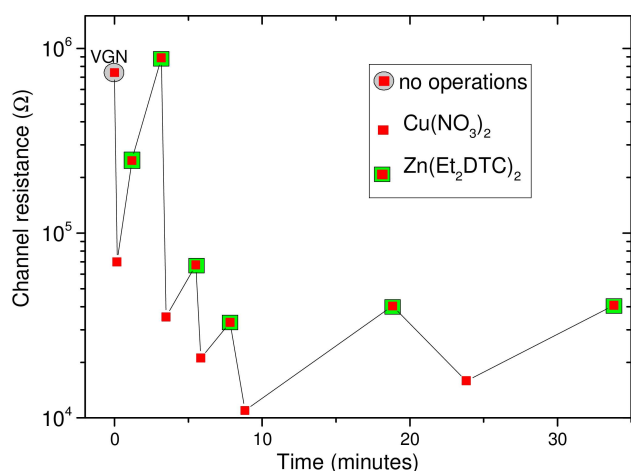

Figure 7. Electrical evaluation of a typical Zn:CdS synaptic device submitted to different operations. The VGN film is set to LRS state using $Cu(NO_3)_2$ and reset to HRS using $Zn(Et_2DTC)_2$ solution.

can be alternately set to LRS and HRS by performing the cationic exchange (Cu^{2+}/Zn^{2+}) as previously discussed. The channel resistance exhibits a logarithmic relationship with dipping time. Notice that LRS activation ($Cu(NO_3)_2$ solution) is faster than the Cu-removal process which reset the device to HRS ($Zn(Et_2DTC)_2$ solution). Probably this effect is due to the polarity of the solvents. For instance, $Cu(NO_3)_2$ is dissolved in methanol which is a polar and protic solvent, like water. On the other hand, zinc diethyldithiocarbamate is dissolved in chloroform, which limits the ionic equilibria (solubility) at the interface between the film and the solvent. The different resistance states, available in our devices may be associated to artificial synapses as previously reported by Gkoupidenis *et al.*[17] using electrochemical transistors. For instance, Gkoupidenis *et al.* activated and deactivated their transistors by sweeping the gate voltage through a liquid electrolyte, which increases/decreases the carrier density in the semiconducting channel. Similarly, our devices are activated (LRS) and deactivated (HRS) by wetting the film with different solutions.

Considerations on the evolution of the resistive parameters Rct and R$_{channel}$

To compare the resistive behavior of the FTO/Zn:CdS devices, electrically characterized through DC measurements, and the results obtained in the Zn:CdS electrode of the electrochemical cell characterized by AC measurements, we have idealized the electrical systems as reported in Figure 8. In AC impedance measurements, the RC response of the system can be considered as the sum of thousands of smaller RC systems distributed all over the film's surface. As discussed above, when
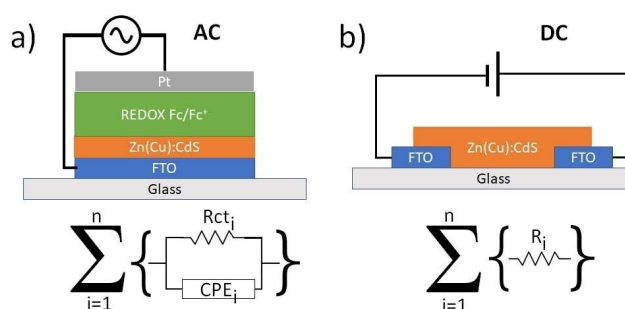
Figure 8. (a) Schematic diagram of the electrochemical cell used for the AC setup. In this configuration the device can be considered as the sum of *n* single RC circuits which represents the charge-transfer process at the interface between electrolyte and electrode. The charge pass through the interface and recombines with the electrolyte generating an RC interface with the resistive element Rct(i) in parallel with a capacitor CPE(i). On the other hand, **(b)** the DC setup can also be idealized as the sum of *n* single resistive elements Ri that constitute the the channel between two FTO electrodes (terminals).

the system is set to LRS the catalytic efficiency, towards FCE is significantly increased, showing a lower time constant (faster reaction) and a lower Rct (Tab.1). On the other hand, successive depletion of Cu^{2+} reduces the number of active-sites on the films surface, leading to an increase of Rct. Notice that pure CuS is a powerful catalyst for the reversible redox pair Fc/Fc$^+$.[38]

The plot of ln(Rct) *vs* dipping-time (Figure 9) shows different slopes before and after 10 minutes. The first 10 minutes of
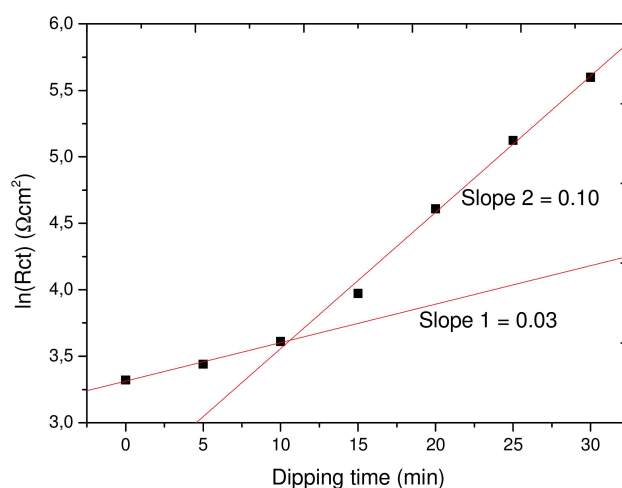
Figure 9. Plot of ln(Rct) *vs* dipping-time of the film in $Zn(Et_2DTC)_2$ dissolved in chloroform. The increase rate of Rct is obtained by two different slopes. The electrochemical setup of this measurement is shown in Figure 8 a).

the Cu$_{(Zn)}$:CdS immersion in the Cu-removal solution presents a slow increase of Rct at a slope = 0.03, while between 10 and 30 minutes the evolution constant shows a higher value, slope = 0.10. This behavior may occur due to combination of two

effects involving the decreasing Cu-content in the film: the electrocatalytic activity and the film resistivity. Notice that most of the conductivity in Cu_xS occurs by diffusion of Cu^{2+} ions through the film.[42] Thus, the first slope can be attributed just to the predominance of the effect on the films electrocatalytic activity towards FCE. The slope increases when the lack of Cu^{2+} is enough to significantly reduce the films resistivity.

On the other hand, using the DC setup, the resistance of the film depends just on the resistivity (ρ), whereas the geometry of the device does not change during the measurement (fixed channel length). As reported by Mohamed *et al.*[43] in a research on Cu-doped ZnS films, the films resistivity was strongly influenced by the copper content. It was also demonstrated considering Cu-doped PbS, where copper was responsible for an effective increase of the charge carriers concentration in the semiconductor, showing a direct effect on its resistivity.[44] Moreover, we noticed a strong logarithmic relationship of the channel resistance as a function of the dipping time into the Cu-removal solution. Therefore, the film resistivity is highly dependent of the overall copper content (Figure 6). Copper may contribute to the conductivity by creating midgap states inside the semiconductor band-gap.[45]

Considering the cation exchange capabilities, discussed in the previous paragraph, in the future the as proposed system could be optimized for the detection of heavy metals like Hg which shows a strong affinity with sulfur, forming insoluble compounds. Nevertheless, future investigations should focus on the replacement of chloroform with a less toxic solvent. Other ion exchange systems could be considered such as Al-doped Fe_2O_3, in which Al as well as Fe could be exchanged by another transition metal with a stronger interaction with oxygen with a similar mechanism. The as-proposed artificial synapse based on Zn:CdS still represents a slow memory system. However, surface engineering could be considered using porous nanostructures with larger surface area to speed-up the ionic exchange.

3. Conclusions

We presented a novel ion exchange memristor which shown a neuromorphic behavior mimicking a synthetic synapse. The memristor is based on thin films of Zn:CdS, with a zinc to cadmium ratio of 10:90. The resistance states are induced by the substitutional exchange of Zn^{2+} by Cu^{2+} driven by different thermodynamics constants of solubility equilibria. The insertion of Cu^{2+} in the film produces a sharp drop of the resistance as well as a higher catalytic activity towards a well-known redox couple (Fc/Fc^+). The absorbed copper can be removed and substituted back by Zn^{2+} by means of a novel chemical reaction never reported so far in the literature, in which a saturated solution of $Zn(Et_2DTC)_2$ reacts with the films surface removing Cu^{2+} ions. Considering the results reported in this work we can conclude that Zn:CdS has potential applications in neuromorphic systems such as *brain on a chip* in which the activating and deactivating solutions flow into a microfluidic system providing the necessary reactants to the active sites of the device.

Supplementary Information Summary

Materials and methods. State transition and RW operations. A feasible way to reprogram the HRS by $Cd(Et_2DTC)_2$. EDS analysis

Conflict of Interest

The authors declare no conflict of interest.

Keywords: Electrochemical · memory · memristors · neuromorphic · synaptic

[1] M. Bushnell, V. Agrawal, Essentials of Electronic Testing for Digital, Memory and Mixed-Signal VLSI Circuits, Springer Science & Business Media, **2004**.
[2] L. Chua, *IEEE Trans. Circuit Theory* **1971**, 18, 507–519.
[3] D. B. Strukov, G. S. Snider, D. R. Stewart, R. S. Williams, *Nature* **2008**, 453, 80–83.
[4] R. Waser, M. Aono, *Nat Mater* **2007**, 6, 833–840.
[5] Y. Yang, S. Choi, W. Lu, *Nano Lett.* **2013**, 13, 2908–2915.
[6] J. Borghetti, G. S. Snider, P. J. Kuekes, J. J. Yang, D. R. Stewart, R. S. Williams, *Nature* **2010**, 464, 873–876.
[7] D. B. Strukov, K. K. Likharev, *Nanotechnology* **2005**, 16, 888–900.
[8] T. Ohno, T. Hasegawa, T. Tsuruoka, K. Terabe, J. K. Gimzewski, M. Aono, *Nat. Mater.* **2011**, 10, 591–5.
[9] M. D. Pickett, G. Medeiros-Ribeiro, R. S. Williams, *Nat. Mater.* **2013**, 12, 114–7.
[10] T. Driscoll, J. Quinn, S. Klein, H. T. Kim, B. J. Kim, Y. V. Pershin, M. Di Ventra, D. N. Basov, *Appl. Phys. Lett.* **2010**, 97.
[11] J. Borghetti, Z. Li, J. Straznicky, X. Li, D. A. A. Ohlberg, W. Wu, D. R. Stewart, R. S. Williams, *Proc. Natl. Acad. Sci. U. S. A.* **2009**, 106, 1699–703.
[12] Q. Xia, W. Robinett, M. W. Cumbie, N. Banerjee, T. J. Cardinali, J. J. Yang, W. Wu, X. Li, W. M. Tong, D. B. Strukov, et al., *Nano Lett.* **2009**, 9, 3640–3645.
[13] M. H. Boratto, R. A. Ramos, M. Congiu, C. F. O. Graeff, L. V. A. Scalvi, *Appl. Surf. Sci.* **2017**, 410.
[14] A. Thomas, *J. Phys. D. Appl. Phys.* **2013**, 46.
[15] Y. Van De Burgt, E. Lubberman, E. J. Fuller, S. T. Keene, G. C. Faria, S. Agarwal, M. J. Marinella, A. A. Talin, *A. Salleo*, **2017**, 1–6.
[16] P. Gkoupidenis, D. A. Koutsouras, G. G. Malliaras, *Nat. Commun.* **2017**, 8, 15448.
[17] P. Gkoupidenis, N. Schaefer, B. Garlan, G. G. Malliaras, *Adv. Mater.* **2015**, 27, 7176–7180.
[18] A. Pestronk, *Neurology* **1997**, 48, 299–300.
[19] J. Konorski, Conditioned reflexes and neuron organization, Cambridge University Press, New York, **1948**.
[20] A. L. Hodgkin, A. F. Huxley, *J. Physiol.* **1952**, 117, 500–544.
[21] L. CHUA, V. SBITNEV, H. KIM, *Int. J. Bifurc. Chaos* **2012**, 22, 1230011.
[22] K. S. Cole, *J. Gen. Physiol.* **1941**, 25, 29–51.
[23] K. S. Cole, R. F. Baker, *J. Gen. Physiol.* **1941**, 24, 771–788.
[24] L. J. Elias, D. M. Saucier, Neuropsychology: Clinical and Experimental Foundations, Pearson/Allyn & Bacon, **2006**.
[25] E. F. Stanley, *J. Neurophysiol.* **2000**, 83, 477–82.
[26] M. Congiu, A. Lanuti, A. di Carlo, C. F. O. Graeff, *Sol. Energy* **2015**, 122, 87–96.
[27] J. O. M. Bockris, B. E. Conway, R. E. White, Modern Aspects of Electrochemistry, Springer US, **2012**.

[28] M. Congiu, L. G. S. Albano, F. Decker, C. F. O. Graeff, *Electrochim. Acta* **2015**, 151, 517–524.

[29] E. Barsoukov, J. R. Macdonald, Impedance Spectroscopy: Theory, Experiment, and Applications, John Wiley & Sons, **2005**.

[30] D. E. Ortiz-Ramos, L. A. Gonzalez, R. Ramirez-Bon, *Mater. Lett.* **2014**, 124, 267–270.

[31] D. A. Tarr, G. L. Miessler, Inorganic Chemistry: Solutions Manual, Prentice Hall, **1999**.

[32] F. A. Cotton, G. Wilkinson, Advanced Inorganic Chemistry, Wiley New York, **1988**.

[33] F. Jellinek, React. Solids **1988**.

[34] H. Orofino, S. P. Machado, R. B. Faria, *Química Nov.* **2013**, 36, 894–896.

[35] X. Shuai, W. Shen, X. Li, Z. Hou, S. Ke, G. Shi, C. Xu, D. Fan, *Mater. Sci. Eng. B Solid-State Mater. Adv. Technol.* **2018**, 227, 74–79.

[36] J. Datta, M. Das, A. Dey, S. Halder, S. Sil, P. P. Ray, *Appl. Surf. Sci.* **2017**, 420, 566–578.

[37] K. Sun, C. Yan, F. Liu, J. Huang, F. Zhou, J. A. Stride, M. Green, X. Hao, *Adv. Energy Mater.* **2016**, 6.

[38] M. Congiu, O. Nunes-Neto, M. L. De Marco, D. Dini, C. F. O. Graeff, *Thin Solid Films* **2016**, 612, 22–28.

[39] J. Labuda, M. Skatulokova, M. Nemeth, S. Gergely, *Chem. Zvesti* **1984**, 38, 597–605.

[40] J. Rivnay, P. Leleux, M. Ferro, M. Sessolo, A. Williamson, D. A. Koutsouras, D. Khodagholy, M. Ramuz, X. Strakosas, R. M. Owens, et al., *Sci. Adv.* **2015**, 1, e1400251–e1400251.

[41] J. A. Pavanello, M. A., Claeys, C., & Martino, Microelectronics Technology and Devices-SBMicro 2010, The Electrochemical Society, Pennington, New Jersey, **2011**.

[42] R. Dong, D. S. Lee, W. F. Xiang, S. J. Oh, D. J. Seong, S. H. Heo, H. J. Choi, M. J. Kwon, S. N. Seo, M. B. Pyun, et al., *Appl. Phys. Lett.* **2007**, 90.

[43] S. H. Mohamed, *J. Phys. D. Appl. Phys.* **2010**, 43, 35406.

[44] X. Zheng, F. Gao, F. Ji, H. Wu, J. Zhang, X. Hu, Y. Xiang, *Mater. Lett.* **2016**, 167, 128–130.

[45] Z. Huang, X. Zou, H. Zhou, *Mater. Lett.* **2013**, 95, 139–141.